

# Determination of the Interaction Between Glimepiride and Hyperbranched Polymers in Solid Dispersions

DAVID PAHOVNIK,<sup>1</sup> SEBASTJAN REVEN,<sup>2</sup> JOŽE GRDADOLNIK,<sup>1,3</sup> ROK BORŠTNAR,<sup>1</sup> JANEZ MAVRI,<sup>1,3</sup> EMA ŽAGAR<sup>1,3</sup>

<sup>1</sup>National Institute of Chemistry, SI-1000 Ljubljana, Slovenia

<sup>2</sup>Lek Pharmaceuticals d.d., Sandoz Development Center Slovenia, SI-1526 Ljubljana, Slovenia

<sup>3</sup>EN-FIST Centre of Excellence, SI-1000 Ljubljana, Slovenia

Received 14 March 2011; revised 19 May 2011; accepted 20 May 2011

Published online 8 June 2011 in Wiley Online Library (wileyonlinelibrary.com). DOI 10.1002/jps.22662

**ABSTRACT:** Solid dispersions of glimepiride, belonging to the sulfonyleurea group of antidiabetic drugs, and poly(ester amide) hyperbranched polymers of different chemical compositions were prepared in order to improve glimepiride's poor water solubility. X-ray powder diffraction results show that glimepiride is in noncrystalline form, indicating that drug molecules are molecularly dispersed within the amorphous hyperbranched polymers. Nuclear magnetic resonance spectroscopy and Fourier transform–infrared spectroscopy results reveal the complex formation between the glimepiride drug and the particular hyperbranched polymer, which was confirmed also by quantum chemical calculations. The complex is stabilized by a hydrogen-bond interaction between the NH group of the sulfonyleurea segment of glimepiride and the carbonyls of the amide and ester bonds of the hyperbranched polymers. The slightly acidic proton of the NH group of the sulfonyleurea segment of glimepiride is also involved in an interaction with the tertiary amino functional groups of the hyperbranched polymer. As a consequence, the loading capacity is higher for the hyperbranched polymer with the tertiary amino groups. Owing to a complex formation between glimepiride and a particular hyperbranched polymer, glimepiride's water solubility and its dissolution rate are considerably improved relative to the pure glimepiride drug. © 2011 Wiley-Liss, Inc. and the American Pharmacists Association *J Pharm Sci* 100:4700–4709, 2011

**Keywords:** solid dispersion; drug interactions; X-ray powder diffractometry; FTIR; NMR spectroscopy; *ab initio* calculation

## INTRODUCTION

The discovery and approval of several new types of oral antidiabetic drugs for the management of type 2 diabetes have resulted in their rapidly increasing use. However, many of these drugs belong to class II of the biopharmaceutical classification system, exhibiting a high permeability and poor water solubility. The low drug bioavailability results in an irreproducible clinical response or even in a therapeutic failure and in a waste of a large portion of the oral dose, which adds to the cost of the drug therapy. Thus, poorly water-soluble drugs provide a challenge when it comes to delivery in an active and absorbable form to the desired site of action.<sup>1</sup> One of the methods used to increase

their solubility and/or dissolution rate is the transformation of the drug from its crystalline form into the amorphous state. However, the amorphous form of the drugs is thermodynamically metastable and often also chemically more unstable than their corresponding crystalline form, which greatly enhances the probability of a physical transformation (recrystallization) and/or a chemical degradation of the amorphous drugs.

To overcome these effects, the solid dispersions of drugs with hydrophilic or amphiphilic polymers are often prepared, in which the polymeric carrier acts as a drug stabilizer and/or a crystallization inhibitor, and in this way preserves the drug in its molecular state.<sup>2–9</sup> Solid dispersions can be prepared by the melting method, the solvent method, or by a combination of both methods.<sup>10–18</sup> The polymers commonly used in the solid dispersion technology are conventional linear polymers such as poly(vinylpyrrolidone),

Correspondence to: E. Žagar (Telephone: +386-1-4760-203; Fax: +386-1-4760-300; E-mail: ema.zagar@ki.si)

*Journal of Pharmaceutical Sciences*, Vol. 100, 4700–4709 (2011)  
© 2011 Wiley-Liss, Inc. and the American Pharmacists Association

poly(methacrylate), various cellulose derivatives, and so on.<sup>19–23</sup> In recent years, dendritic polymers (dendrimers, hyperbranched polymers, dendronized polymers, dendrigrafts, etc.) have attracted a lot of attention for their use in biomedical applications<sup>24–28</sup> because they exhibit a number of properties that differentiate them from the conventional linear polymers, and that results from their unique branched architecture and a large number of functional groups.<sup>29–33</sup> As a result, the dendritic polymers in solution form unimolecular micelles, the structure of which is similar to that of the conventional micelles made of amphiphilic linear block copolymers; only the unimolecular micelles consist of covalently bound chains, whereas the chains of the conventional micelles are bound together through physical bonds. Therefore, the formation and stability of the unimolecular micelles are independent of thermodynamic factors such as the solution concentration and temperature. Active pharmaceutical ingredients can physically interact with dendritic polymers through either encapsulation into dendritic interior void spaces (nanoscale container) or association with surface functional groups (nanoscaffolding), or a mixture of both. The driving forces for these interactions can be hydrogen bonding, van der Waals interactions, or the electrostatic interaction between the opposite charges on the dendritic polymers and the drug.<sup>34</sup>

In our previous work, we studied the feasibility of using hyperbranched polymers, that is, commercially available poly(ester amide)s with hydroxyl and tertiary amine functional groups with the trade names Hybrane S1200 and Hybrane HA1690, respectively, as the solubilization enhancers for the poorly water-soluble oral antidiabetic drug called glimepiride.<sup>35</sup> Glimepiride belongs to the third generation of sulfonylurea drugs and is useful for the management of diabetes mellitus of type 2. In addition to its poor solubility (~5 mg/L at pH value of 7.4), it also shows a slow dissolution rate and a pH dependent solubility.<sup>36</sup> The results of our study revealed that the preparation of solid dispersions of glimepiride with poly(ester amide) hyperbranched polymers using a solvent method results in a significantly enhanced aqueous solubility and dissolution rate of the glimepiride drug,<sup>35</sup> which was ascribed to the molecularly dissolved glimepiride within the solid dispersions.

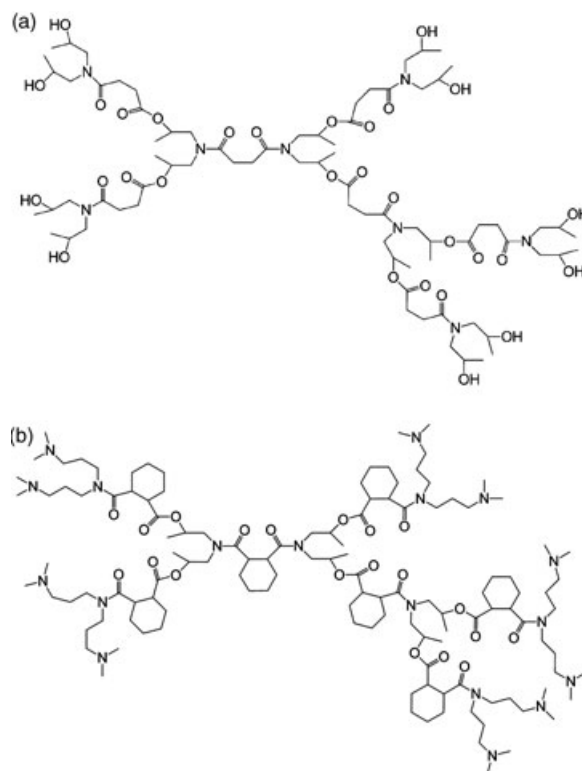
The aim of the present investigation was to exactly determine the type of interactions between the glimepiride drug and the particular hyperbranched polymer in the solid dispersion because these specific interactions are responsible for the formation of a stable complex and, consequently, for the improved glimepiride solubility as well as dissolution rate. The morphology of glimepiride within solid dispersions was determined by X-ray powder diffraction (XRD)

and differential scanning calorimetry (DSC) analyses, whereas the interactions between the drug and the drug carrier were experimentally investigated using nuclear magnetic resonance (NMR) spectroscopy and Fourier transform infrared (FTIR) spectroscopy. The interaction energies between glimepiride and a particular hyperbranched polymer were also calculated using quantum chemical calculations.

## MATERIALS AND METHODS

### Materials

Glimepiride, (1-[4[2-(3-ethyl-4-methyl-2-oxo-3-pyrroline-1-carboxamide)ethyl] phenyl sulphonyl]-3-*trans*-4-methylcyclohexyl)urea, was supplied in crystalline form by Glenmark (Mumbai, India). Hyperbranched poly(ester amide)s, that is, Hybrane S1200 with hydroxyl functional groups and Hybrane HA1690 with tertiary amine functional groups (Scheme 1), were obtained from DSM (Sittard, The Netherlands). The solvents and chemicals used for the preparation and characterization of the solid dispersions were all of analytical grade and supplied by Merck (Darmstadt, Germany).



**Scheme 1.** Schematic presentation of hyperbranched polymers containing (a) hydroxyl and (b) tertiary amine functional groups.

## Preparation of Solid Dispersions

For the preparation of the solid dispersions using a solvent method, glimepiride and the hyperbranched polymer were dissolved in 96% ethanol at room temperature during continuous stirring with a magnetic stirrer (RT 10 Power; IKA Werke, Staufen, Germany) at a speed of 480 rpm for 1 h to assure transparent solution. The solvent was removed at slightly elevated temperature (40°C) in a vacuum (Heraeus vacuotherm VT 6025; Thermo Scientific, Waltham, Massachusetts, USA) and then dried for 3 days at the same conditions. The weight ratios of glimepiride and the hyperbranched polymers in the solid dispersions were 5:95 and 9:91 in the cases of the solid dispersions based on Hybrane S1200 and Hybrane HA1690, respectively.

The physical mixtures of glimepiride and a particular hyperbranched polymer were prepared in a dry box. Glimepiride and hyperbranched polymer were mixed and grinded in an appropriate weight ratio in a mortar with pestle to ensure the preparation of a homogeneous mixture.

## X-Ray Powder Diffraction

The X-ray patterns were recorded on a X-ray powder diffractometer PANalytical X'Pert PRO MPD (Almelo, The Netherlands). The samples were exposed to Cu K $\alpha$ 1 = 1.5406 Å radiation in 0.04° steps from 2 $\theta$  = 5° to 30°.

## NMR Spectroscopy

The <sup>1</sup>H and <sup>13</sup>C NMR spectra were recorded on a Varian Unity Inova 300 instrument (Oxford, UK) in the pulse Fourier transform mode. The relaxation delay and the acquisition time for the <sup>1</sup>H NMR were both 5 s, and for the <sup>13</sup>C NMR, they were 2 s. The samples were dissolved in DMSO-*d*<sub>6</sub> and tetramethylsilane was used as an internal standard.

## Differential Scanning Calorimetry

The differential scanning calorimetric measurements were made on a PerkinElmer Pyris 1 calorimeter (Waltham, Massachusetts, USA). For determination of the glass transition temperature, the samples were first cooled to -50°C and then heated to 150°C at 20°C/min (first heating scan). After that, the samples were cooled at a rate of 200°C/min back to -50°C (first cooling scan) and reheated back to 150°C at 20°C/min (second heating scan). The glass transition temperature was determined from the second heating scan.

For the detection of the presence of crystalline glimepiride in the solid dispersions, separate experiments were performed where the solid dispersions were first cooled to -50°C and then heated to 230°C at 10°C/min.

## Fourier Transform–Infrared Spectroscopy

The infrared spectra were recorded on a Perkin Elmer System 2000 spectrometer (Waltham, Massachusetts, USA). Typically, 256 scans were averaged and apodized with triangular functions at a nominal resolution of 2 cm<sup>-1</sup>. The spectra were measured at room temperature in attenuated total reflectance (ATR) mode on a Specac Golden Gate ATR cell (Riverhouse, UK) equipped with a diamond crystal. The ATR spectra were used without additional processing, such as corrections due to the frequency dependent depth of penetration or spectral anomalies due to reflection.

## Stability Studies of the Solid Dispersions

The physical stability of glimepiride in solid dispersions was evaluated at 25°C and 80% relative humidity (RH). Saturated salt solution of ammonium bromide was used to maintain 80% RH in the respective chamber at 25°C. Additionally, the samples were also closed in vials and stored in refrigerator (2–8°C). The samples were removed after 7 days.

*In vitro* dissolution study was performed in order to detect the possible change in glimepiride dissolution profile that could result from the influence of elevated humidity on glimepiride partial recrystallization. *In vitro* dissolution studies were performed in phosphate buffer solution at pH = 6.8, physiologically relevant media, at 37°C using a USP Dissolution Tester, Apparatus II (Paddle method) (Varian 705 DS, Cary, North Carolina, USA) at a rotation rate of 75 rpm. The tested samples were added in the correct amount directly to 900 mL phosphate buffer solution to achieve a final glimepiride concentration of 4.4 µg/mL, which equals the concentration of therapeutic dose dissolved in 900 mL. Experiments were performed in triplicates. Aliquots, each of 2 mL, were withdrawn from the dissolution medium at time intervals of 5, 15, 30, 60, and 120 min. The sample aliquots were withdrawn through a syringe and filtered through a Millipore filter (0.45 µm, Polyvinylidene fluoride, Billerica, Massachusetts, USA). The sample aliquots were analyzed for the dissolved glimepiride content using reversed-phase high-performance liquid chromatography (HPLC) method.

The amount of dissolved glimepiride was estimated by reversed-phase HPLC (Waters Alliance, Milford, Massachusetts, USA) in a binary mode with a photodiode array detector at 230 nm. The analysis were performed on a C18 column (150 × 4.6 mm<sup>2</sup>, 3.5 µm) placed in a column oven at 30°C and a mobile phase: A [phosphate buffer (pH 2.5)–acetonitrile (72:28)] and B [phosphate buffer (pH 2.5)–acetonitrile (30:70)] delivered at a flow rate of 1.5 mL/min under the following gradient conditions: 0–6 min (100% A to 0% A), 6–6.5 min (0% A–100% A). The column

equilibration time was 5 min. The retention time of glimepiride was 4.0 min. The concentration of the dissolved glimepiride was determined from the area of glimepiride peak using preformed calibration curve. Standard curve for glimepiride was measured over a range of 15 to 0.1  $\mu\text{g/mL}$  and was shown to be linear. The limit of glimepiride detection was 0.005  $\mu\text{g/mL}$ .

### Quantum Chemical Calculations

The quantum chemical calculations were performed on an 8-core AMD-based workstation (Sunnyvale, California, USA). The *ab initio* HF/STO-3G and HF/6-31G(d) calculations were performed using the Gaussian09 suite of programs (Wallingford, Connecticut, USA).<sup>37</sup> The size of the system did not allow more flexible basis sets and inclusion of electron correlation.<sup>38,39</sup> The interaction energy was calculated by using the method of supermolecules as the difference between the energy of the complex minus the energy of the hyperbranched polymer, minus the energy of glimepiride. Zero-point corrections were considered.

The solvation free energies of the hyperbranched polymer, glimepiride, and the complex were calculated using the Langevin dipoles model parametrized by Florian and Warshel.<sup>40</sup> The Merz–Kollman partial atomic charges were calculated on the HF/STO-3G and HF/6-31G(d) level of theory.

In order to define the acidic proton of glimepiride, we used the established quantum chemical procedures for calculating the *pK<sub>a</sub>* values discussed in a previous publication and the references therein.<sup>41</sup> Zero-point corrections were considered.

## RESULTS AND DISCUSSION

### XRD and DSC Studies

In our previous study, X-ray diffraction analyses were used to assess the presence of crystalline glimepiride or its polymorph modifications within the prepared solid dispersions.<sup>35</sup> However, the peaks that would indicate the presence of crystalline glimepiride were absent in the X-ray diffraction patterns of the solid dispersions; only a broad amorphous halo typical for amorphous hyperbranched polymers was seen up to a certain glimepiride concentration, that is, 5 and 9 wt % for the hyperbranched polymers containing hydroxyl and amino functional groups, respectively (Fig. 1). To make sure that the content of the amorphous glimepiride in the solid dispersions is not below the detection limit, we also made X-ray measurements on physical mixtures of glimepiride and the particular hyperbranched polymer in the same weight ratio as that in the corresponding solid dispersions (Fig. 1). The X-ray patterns of the physical mixtures show sharp peaks superimposed on an amorphous

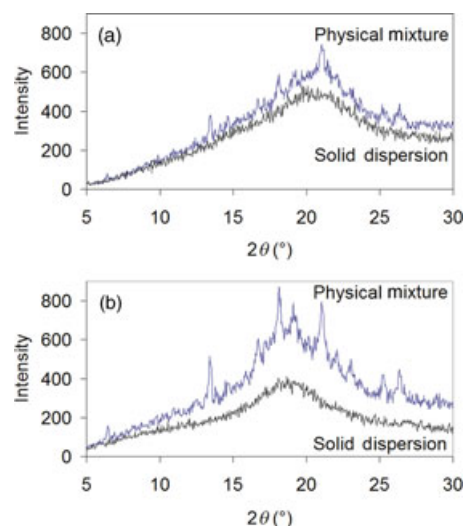


**Figure 1.** X-ray powder diffractograms of the physical mixture and the solid dispersion containing (a) 5 wt % of glimepiride and 95 wt % of hyperbranched polymer consisting of functional hydroxyl groups and (b) 9 wt % of glimepiride and 91 wt % of hyperbranched polymer consisting of tertiary amino functional groups.

halo. These signals are due to the presence of the crystalline glimepiride. The signal intensity of the crystalline glimepiride is higher in the X-ray pattern of the physical mixture consisting of the glimepiride and the hyperbranched polymer terminated with amino functional groups than the signal intensity in the X-ray pattern of the physical mixture of glimepiride and the hyperbranched polymer terminated with hydroxyl functional groups because the drug content is higher in the former case. Similar X-ray patterns to those of the physical mixtures were also obtained with the solid dispersions, in which the glimepiride concentration in the solid dispersion with the hyperbranched polymer consisting of hydroxyl and amino groups exceeds 5 and 9 wt %, respectively.<sup>35</sup>

On the basis of these results, we concluded that during the solvent evaporation, glimepiride does not crystallize up to a certain concentration, which depends on the chemical composition of the hyperbranched polymer used for the preparation of the solid dispersion. The noncrystalline form of glimepiride within the solid dispersions indicates molecularly dispersed drug molecules within the amorphous hyperbranched polymers. Such system is called an amorphous solid solution.<sup>9</sup> Glimepiride specifically interacts with poly(ester amide) hyperbranched polymers, which is also the reason for its improved water solubility. Above these limiting concentrations, which equal the maximum loading capacities of particular hyperbranched polymers, glimepiride crystallizes as a separate solid phase during the solvent evaporation.<sup>35</sup>

The DSC thermograms of the hyperbranched polymers and the solid dispersions show only a broad glass

transition temperature due to the amorphous hyperbranched polymers. The glass transition temperature of the pure hyperbranched polymer containing amino functional groups ( $T_g = 23.1^\circ\text{C}$ ) is comparable to that of the solid dispersion consisting of glimepiride and this polymer ( $T_g = 22.5^\circ\text{C}$ ), whereas the glass transition temperature of the pure hyperbranched polymer containing hydroxyl functional groups ( $T_g = 45.6^\circ\text{C}$ ) is higher than that of the solid dispersion based on it ( $T_g = 35.0^\circ\text{C}$ ). The lower glass transition temperature of the solid dispersion based on hyperbranched polymer containing hydroxyl groups as compared with the pure hyperbranched polymer was ascribed to a plasticizing effect of the drug molecules.<sup>9</sup> The differential infrared spectroscopy also shows that the hydrogen-bond network in the hyperbranched polymer rearranges during the preparation of the solid dispersion toward the less hydrogen bonded network, which could also result in reduced glass transition temperature.<sup>42</sup> On the contrary, the glass transition temperature of the hyperbranched polymer containing tertiary amino functional groups is not affected significantly by the solid dispersion preparation, indicating less plasticizing effect of the drug. In addition, this hyperbranched polymer contains only proton acceptors and no proton donor groups in the structure and as a result, it does not form a hydrogen-bond network.

The DSC curves of both hyperbranched polymers show the onset of thermal decomposition at temperatures of  $120^\circ\text{C}$  and  $150^\circ\text{C}$  for the hyperbranched polymer consisting of hydroxyl and amino functional groups, respectively. This is the reason why the presence of the crystalline glimepiride with a melting point at  $214^\circ\text{C}$  cannot be determined from their DSC thermograms, neither in the solid dispersions nor in the physical mixtures.

### $^1\text{H}$ NMR and $^{13}\text{C}$ NMR Spectroscopic Studies

The type of interaction between glimepiride and the poly(ester amide) hyperbranched polymers in the form of solid dispersions were studied by proton and carbon NMR as well as by IR spectroscopy.

The assigning of the glimepiride signals in the proton NMR spectra,  $^1\text{H}$  NMR (300 MHz,  $\text{DMSO-}d_6$ )  $\delta$  (ppm) is as follows: 10.32 (s, 1H), 8.37 (t,  $J = 5.7$  Hz, 1H), 7.81 (d,  $J = 8.5$  Hz, 2H), 7.46 (d,  $J = 8.5$  Hz, 2H), 6.28 (d,  $J = 7.8$  Hz, 1H), 4.17 (s, 2H), 3.50 (dq,  $J = 7.1$ , 6.3 Hz, 2H), 3.22–3.13 (m, 1H), 2.90 (t,  $J = 7.1$  Hz, 2H), 2.19 (q,  $J = 7.6$  Hz, 2H), 1.71–1.57 (m, 4H), 1.34–1.19 (m, 1H), 1.16–1.03 (m, 2H), 0.98 (t,  $J = 7.6$  Hz, 3H), 0.94–0.86 (m, 2H), 0.82 (d,  $J = 6.5$  Hz, 3H).

Figure 2 shows magnified regions of the  $^1\text{H}$  NMR spectra of pure glimepiride and its solid dispersions with hyperbranched polymers containing the hydroxyl and amine functional groups, respectively (Fig. 2). The displayed regions represent only the sig-

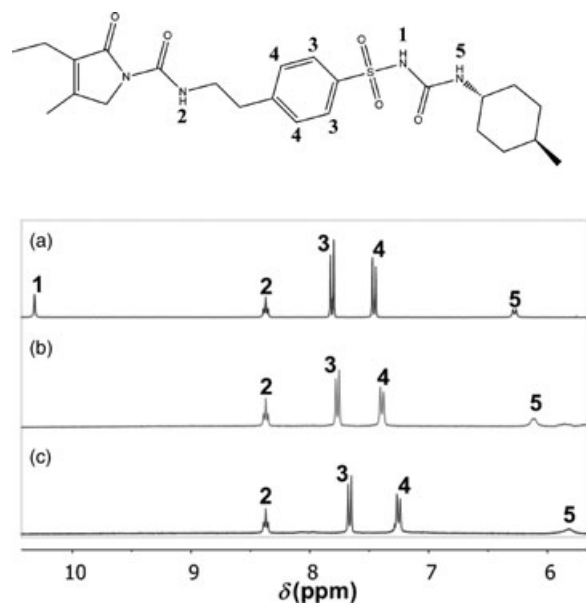


**Figure 2.** Magnified  $^1\text{H}$  NMR spectra of (a) glimepiride and its solid dispersions with hyperbranched polymers containing the (b) hydroxyl and (c) the tertiary amino functional groups.

nals belonging to the glimepiride drug whose chemical shifts are the most affected by the interactions with the hyperbranched polymers. In the spectrum of pure glimepiride, the signal due to the acidic sulfonyleurea proton (marked with the number 1) appears at the chemical shift of 10.32 ppm. In the proton NMR spectra of both solid dispersions, this signal becomes a very wide one, spreading across several ppm. In addition, the signals assigned to the second proton of the sulfonyleurea group (5) and to the phenyl protons (3 and 4) shift slightly to a higher magnetic field. The shifting of the glimepiride signals is more pronounced if it is in the form of a solid dispersion with a hyperbranched polymer consisting of tertiary amine functional groups. Such signal shifting is the consequence of an electron-density rearrangement in the glimepiride structure, resulting from interactions of glimepiride with the hyperbranched polymers. These results, thus, imply that the NH group of the sulfonyleurea segment of glimepiride interacts with the hyperbranched polymers most probably through hydrogen bonding.

On the contrary, a chemical shift of the signal due to the 2-oxo-3-pyrroline-1-carboxamide group (2) in glimepiride is the same regardless of whether glimepiride is in pure form or in the form of solid dispersions with hyperbranched polymers, suggesting that this group does not participate in the interaction with the hyperbranched polymers.

The assigning of the glimepiride signals in the carbon NMR spectra,  $^{13}\text{C}$  NMR (75 MHz,  $\text{DMSO-}d_6$ )  $\delta$  (ppm) is as follows: 12.71, 12.82, 16.01, 22.01,

31.22, 32.29, 33.37, 35.19, 40.03, 48.56, 51.89, 127.33, 129.16, 131.95, 138.20, 144.94, 150.48, 151.65, 151.98, 171.81.

Magnified regions of the  $^{13}\text{C}$  NMR spectra show a shifting of the signals of the glimepiride sulfonylurea carbonyl group (4) as well as the signals of the aromatic ring (signals denoted as 5, 6, 8, and 9) if glimepiride is in the form of the solid dispersions (Fig. 3). On the contrary, the chemical shifts of the signals of the carbonyl groups in the 2-oxo-3-pyrroline-1-carboxamide segment (1 and 2) and the signals of the double bond (3 and 7) do not change significantly (Fig. 3). These results again indicate that the glimepiride sulfonylurea group is the one that interacts with the hyperbranched polymers.

We were not able to determine the groups of the hyperbranched polymers that are involved in the interaction with glimepiride, neither from the proton nor from the  $^{13}\text{C}$  NMR spectra of the solid dispersions because the signals of the hyperbranched polymers are

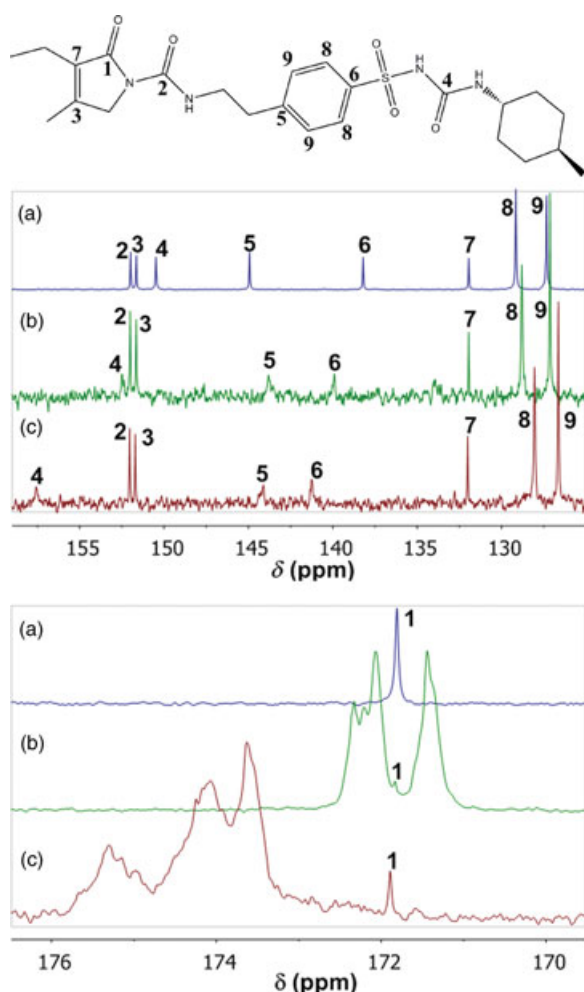


**Figure 3.** Magnified  $^{13}\text{C}$  NMR spectra of (a) glimepiride and its solid dispersions with hyperbranched polymers containing (b) the hydroxyl and (c) the tertiary amino functional groups.

very wide in comparison with the glimepiride signals. Owing to the low glimepiride content in the solid dispersions, the number of polymeric groups involved in the interaction with glimepiride is also small. In addition, the signals indicating the interacting groups of the hyperbranched polymers most probably overlap with those that are not involved in the interaction with glimepiride.

### Infrared Spectroscopic Studies

To ascertain which groups of the hyperbranched polymers interact with the acidic NH group of the sulfonylurea segment of glimepiride, we performed IR spectroscopic measurements in ATR mode. The spectra of the pure hyperbranched polymers were subtracted from the spectra of the solid dispersions to obtain difference spectra, which show the most prominent changes due to the interactions between glimepiride and the hyperbranched polymers (Fig. 4).

The difference spectra reveal a broad absorption located at  $\sim 2010$  and  $\sim 2350\text{ cm}^{-1}$  for the solid dispersions of glimepiride and the hyperbranched polymers containing hydroxyl and tertiary amine functional groups, respectively (Fig. 4). This broad absorption was ascribed to the NH stretching vibration of the sulfonylurea segment in glimepiride. Significant broadening and shifting of the NH stretching band to lower wave numbers

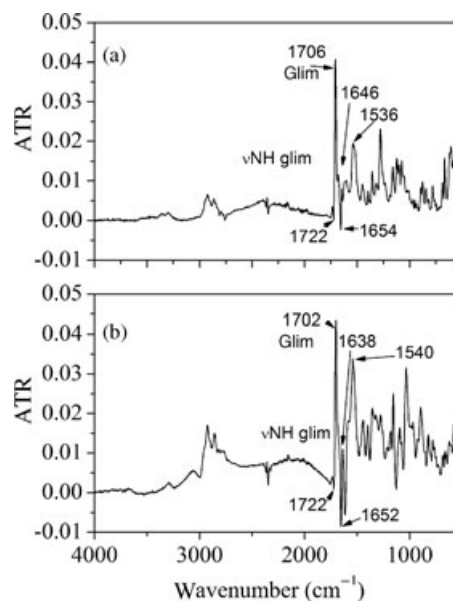


**Figure 4.** The difference spectra of the solid dispersions of glimepiride and the hyperbranched polymer containing (a) the hydroxyl groups and (b) the tertiary amino groups. The difference spectra were obtained by subtraction of the spectra of the pure hyperbranched polymers from the spectra of the solid dispersions. The ATR spectra of the pure hyperbranched polymers were recorded on samples that were prepared under the same conditions as solid dispersions, only without the presence of the glimepiride drug.

is indicative of the formation of medium-to-strong hydrogen bonds in which the NH groups act as proton donors. Moreover, the larger frequency shift of the glimepiride NH stretching vibration for the solid dispersion based on the hyperbranched polymer consisting of tertiary amino functional groups in comparison with the hyperbranched polymer with hydroxyl functional groups suggests that glimepiride forms shorter and stronger hydrogen bonds with the former polymer. The results of the IR spectroscopic studies are thus in agreement with the NMR results.

The carbonyl regions of both difference spectra show red shifts of the  $\nu(\text{O})-\text{C}=\text{O}$  and  $\nu(\text{N})-\text{C}=\text{O}$  bands (Fig. 4). The appearance of negative and positive bands results from the frequency downfield shift of the carbonyl stretching vibration of the ester and amide bonds in the hyperbranched polymers. Such frequency shifts suggest that the carbonyl groups serve as the proton acceptors in  $\text{N}-\text{C}=\text{O}\cdots\text{HN}$  and  $\text{O}-\text{C}=\text{O}\cdots\text{HN}$  hydrogen-bond formation.<sup>35</sup> The intensity ratio of these bands implies a higher relative amount of  $\text{N}-\text{C}=\text{O}\cdots\text{HN}$  as compared with the  $\text{O}-\text{C}=\text{O}\cdots\text{HN}$  hydrogen bonds in the solid dispersion of glimepiride and the hyperbranched polymer containing the amino functional groups.

In addition to the hydrogen bonds, another type of interaction, that is, a proton transfer from the glimepiride sulfonylurea NH group to the tertiary amino group of the hyperbranched polymer, is expected to occur in the case of a solid dispersion of glimepiride and the hyperbranched polymer consisting of tertiary amino groups. In a difference spectrum, this type of interaction should be characterized by the bands that would indicate a stretching  $\text{NH}^+$  vibration between 2700 and 2250  $\text{cm}^{-1}$ , and the antisymmetric and symmetric deformation of the  $\text{NH}^+$  groups located at 1640 and 1620  $\text{cm}^{-1}$  and at 1535 and 1510  $\text{cm}^{-1}$ .<sup>43</sup> The stretching vibration of the  $\text{NH}^+$  groups could coincide with the broad absorption of the NH stretching vibration ( $\sim 2350 \text{ cm}^{-1}$ ) of the glimepiride sulfonylurea segment involved in hydrogen bonding, whereas the identification of the deformation vibrations of the  $\text{NH}^+$  groups is, due to their strong overlapping with more intense bands of glimepiride and polymer vibrations, very difficult. However, strong evidence for this type of interaction is given by the different intensity ratios of the glimepiride bands at 1706 (1702) and 1536 (1540)  $\text{cm}^{-1}$  in both difference spectra, which most probably results from the overlapping of the glimepiride band at 1540  $\text{cm}^{-1}$  and the band due to the deformation vibration of the  $\text{NH}^+$  group at 1535  $\text{cm}^{-1}$ .

The observed changes in the infrared spectra of the solid dispersions imply the existence of hydrogen bonds between the glimepiride NH groups and the carbonyls of the amide and ester groups of the hyperbranched polymers. Besides the interac-

tion of glimepiride with the hyperbranched polymers through hydrogen bonding, glimepiride most probably also interacts with the tertiary amino functional groups of the hyperbranched polymer.

### Stability Studies of the Solid Dispersions

Chemical and physical stability of glimepiride in the solid dispersion, based on hyperbranched polymer with hydroxyl functional groups, which was incorporated into a final tablet solid dosage form (uncoated and coated), was investigated in our previous work.<sup>44</sup> A direct-compression tableting technique was applied for the preparation of the tablets consisting of solid dispersion, lactose, and magnesium stearate (uncoated tablets). Tablets were additionally coated with hydroxypropyl methylcellulose phthalate in order to protect the extremely hygroscopic solid dispersion from atmospheric moisture (coated tablets). The results of stability studies showed that glimepiride is chemically stable if the solid dispersion is incorporated into tablets (coated and uncoated), even if exposed to elevated temperature and/or moisture. *In vitro* dissolution studies of tablet cores show some impact of stress storage conditions (exposure of tablets to high temperature and high humidity for 1 month) on the tablet disintegration time and, consequently, on the drug release rate. Glimepiride solubility also deteriorates somewhat, most probably due to its partial recrystallization. On the contrary, stress storage conditions affect much less the physical stability of glimepiride in tablets coated with hydroxypropyl methylcellulose phthalate, which was ascribed to reduced tablet hygroscopicity due to the presence of protecting coating.

In this work, we tested the physical stability of glimepiride in both solid dispersions, which become deliquescent if they are exposed to humidity because poly(ester amide) hyperbranched polymers are extremely hygroscopic. In these experiments, the solid dispersions were stored in closed vials in a refrigerator for 7 days and in an exicator with 80% RH at room temperature. The results of *in vitro* dissolution studies indicate that both solid dispersions stored in the closed vials in the refrigerator were stable. At the end point of the dissolution study (120 min), the concentrations of the dissolved glimepiride reaches the values close to those determined for the initial solid dispersions, that is, 99% and 98% for solid dispersions based on hyperbranched polymer consisting of hydroxyl and tertiary amine functional groups, respectively (Fig. 5). On the contrary, the solid dispersions stored in the exicator at room temperature and 80% RH show significantly reduced glimepiride solubility because the absorbed moisture most probably competes with glimepiride for hydrogen bonding. In addition, water acts as a plasticizer, which reduces the glass transition temperature of the solid

dispersions and thus, further contributes to complex instability. The results also reveal that the deterioration of glimepiride solubility was much more pronounced for the solid dispersion based on hyperbranched polymer containing hydroxyl functional groups (after 120 min dissolution time, glimepiride solubility was only about 44% of that for the initial solid dispersion) than for the solid dispersion based on the hyperbranched polymer containing tertiary amine functional groups (after 120 min dissolution time, glimepiride solubility was about 84% of that for the initial solid dispersion), which is ascribed to dif-

ferent types of interaction between glimepiride and particular hyperbranched polymer (Fig. 5.).

### Quantum Chemical Calculations

It was experimentally determined that glimepiride has a  $pK_a$  value of 7.26 or 8.07, depending on the method of measurement.<sup>36</sup> These  $pK_a$  values indicate that the aqueous solubility of glimepiride increases with an increasing pH value. The  $pK_a$  values of glimepiride were also calculated in order to determine the most acidic proton of the glimepiride drug. The results of our calculations are in good agreement with the experimental results reported by Grbic et al.,<sup>36</sup> especially those calculated on the HF/6-31G(d) ( $pK_a$  value of 7.96) and HF/6-311++G(2d,2p) ( $pK_a$  value of 7.29) level of theory. The results also reveal that the hydrogen atom in the sulfonylurea segment of glimepiride is an acidic proton and, therefore, the most probable candidate for involvement in hydrogen bonding or to be detached.

For the hyperbranched polymer containing the tertiary amine functional groups, the calculated energy of the hydrogen-bond formation between the sulfonylurea NH group of glimepiride and the carbonyl group of the amide bond ( $N-C=O\cdots HN$ ) is  $-22.58$  kcal/mol and that of the hydrogen bond between the sulfonylurea NH group of glimepiride and the carbonyl group of the ester bond ( $O-C=O\cdots HN$ ) is  $-11.71$  kcal/mol on the HF/6-31G(d) level of theory (Table 1). These results are in agreement with the IR results, showing that the hyperbranched polymer containing the tertiary amine functional groups form more stable (stronger)  $N-C=O\cdots HN$  than  $O-C=O\cdots HN$  hydrogen bonds with glimepiride. The calculations also show that protonation of the tertiary amino functional groups in the hyperbranched polymer by the acidic sulfonylurea proton of glimepiride is also a possible interaction because the free energy of this interaction equals  $-19.62$  kcal/mol on the HF/6-31G(d) level of theory (Table 1).

For the hyperbranched polymer containing the hydroxyl functional groups, the calculated energies of the hydrogen-bond formation between the

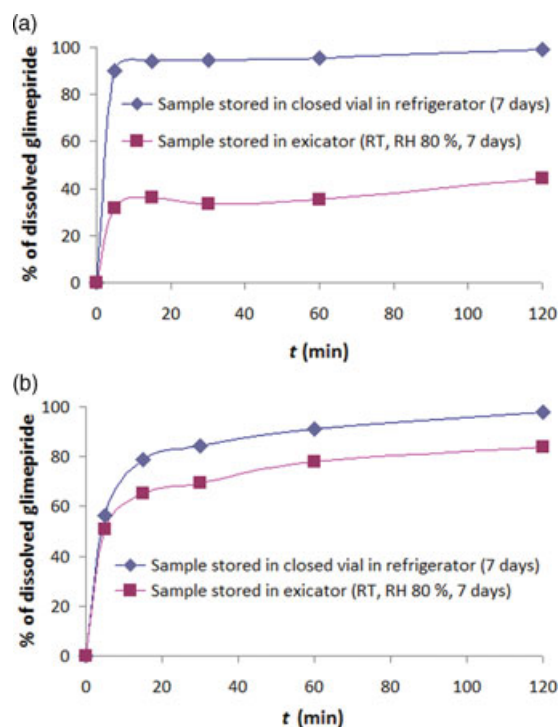


**Figure 5.** Dissolution profiles of solid dispersions based on hyperbranched polymers containing (a) hydroxyl groups and (b) tertiary amino groups, which were stored under different conditions. The results are presented relative to the glimepiride solubility of initial solid dispersion after 120 min dissolution time.

**Table 1.** Interaction Energies  $\Delta G_{\text{assoc}}$  (Free Energies of Association) for Different Types of Interactions Between Glimepiride and Particular Poly(Ester Amide) Hyperbranched Polymer Calculated on the HF/STO-3G and HF/6-31G(d) Level of Theory

Method	Complex of Glimepiride and Polymer with Hydroxyl Groups $\Delta G_{\text{assoc}}$ [kcal mol <sup>-1</sup> ]		Complex of Glimepiride and Polymer with Amine Groups $\Delta G_{\text{assoc}}$ [kcal mol <sup>-1</sup> ]	
	HF/STO-3G	HF/6-31G(d)	HF/STO-3G	HF/6-31G(d)
$N-C=O\cdots HN$	-19.54	-22.87	-19.65	-22.58
$O-C=O\cdots HN$	-28.34	-31.52	-10.21	-11.71
$NH^+$			-17.10	-19.62

Zero point corrections were considered.

$N-C=O\cdots HN$  represents hydrogen bond between amide  $C=O$  group of hyperbranched polymer and  $HN$  of sulfonylurea group of glimepiride.

$O-C=O\cdots HN$  represents hydrogen bond between ester  $C=O$  group of hyperbranched polymer and  $HN$  of sulfonylurea group of glimepiride.

$NH^+$  represents proton transfer from  $NH$  of sulfonylurea group of glimepiride to tertiary amine functional group of hyperbranched polymer.

sulfonylurea NH group of glimepiride and the carbonyl groups of the amide and ester bonds are  $-22.87$  ( $\text{N}-\text{C}=\text{O} \cdots \text{HN}$ ) and  $-31.52$  kcal/mol ( $\text{O}-\text{C}=\text{O} \cdots \text{HN}$ ) on the HF/6-31G(d) level of theory (Table 1), respectively, implying that the carbonyl groups of the ester bonds form somewhat stronger hydrogen bonds with glimepiride than with the amide bonds.

## CONCLUSIONS

In solid dispersions of glimepiride with poly(ester amide) hyperbranched polymers consisting of hydroxyl and tertiary amino functional groups, glimepiride is in an amorphous form up to a concentration of 5 and 9 wt %, respectively. Glimepiride is dispersed on a molecular level within the amorphous hyperbranched polymer. The system is stabilized by a specific interaction between the drug and the hyperbranched polymer. The driving force for the interaction is the hydrogen bonding between the proton of the NH group of the sulfonylurea segment of glimepiride and the carbonyl groups of the amide and ester bonds of the hyperbranched polymers. In the hyperbranched polymer consisting of tertiary amino functional groups, besides hydrogen bonding, a proton transfer from the acidic NH group of the sulfonylurea segment of glimepiride to the tertiary amino group is also a possible driving force for the complex formation, as indicated by experimental results as well as by computational studies. Consequently, the loading capacity of the hyperbranched polymer with tertiary amino functional groups is higher than that with the hydroxyl functional groups. As a result of a complex formation, glimepiride's solubility and its dissolution rate are considerably improved in comparison with the pure glimepiride drug.

## ACKNOWLEDGMENTS

The authors gratefully acknowledge the financial support of Lek Pharmaceuticals d.d., Sandoz Development Center Slovenia, the Ministry of Higher Education, Science and Technology of Republic of Slovenia, and the Slovenian Research Agency (research project #J2-2078).

## REFERENCES

- Seedher N, Kanojia M. 2009. Co-solvent solubilization of some poorly soluble antidiabetic drugs. *Pharm Dev Technol* 14:185–192.
- Hilden RL, Morris KR. 2004. Physics of amorphous solids (minireview). *J Pharm Sci* 93:3–12.
- Gao P. 2008. Amorphous pharmaceutical solids: Characterization, stabilization and development of marketable formulations of poorly soluble drugs with improved oral absorption. *Mol Pharm* 5:903–904.
- Fujii M, Okada H, Shibata Y, Teramachi H, Kondoh M, Watanabe Y. 2005. Preparation, characterization, and tableting of a solid dispersion of indomethacin with crospovidone. *Int J Pharm* 293:145–153.
- Shavi VG, Kumar AR, Usha YN, Armugam K, Ranjan OP, Ginjupalli K, Pandey S, Udupa N. 2010. Enhanced dissolution and bioavailability of gliclazide using solid dispersion techniques. *Int J Drug Deliv* 2:49–57.
- Leonardi D, Barrera MG, Lamas MC, Salomon CJ. 2007. Development of Prednisone: Polyethylene glycol 6000 fast-release tablets from solid dispersions. *AAPS PharmSciTech* 8:221–228.
- Pathak D, Dahiya S, Pathak K. 2008. Solid dispersion of meloxicam: Factorially designed dosage form for geriatric population. *Acta Pharm* 58:99–110.
- Kalava BS, Demirel M, Yazan Y. 2005. Physicochemical characterization and dissolution properties of cinnarizine solid dispersions. *Turkish J Pharm Sci* 2:51–62.
- Leuner C, Dressman J. 2000. Improving drug solubility for oral delivery using solid dispersions. *Eur J Pharm Biopharm* 50:47–60.
- Dhirendra K, Lewis S, Udupa N, Atin K. 2009. Solid dispersions: A review. *Pak J Pharm Sci* 22:234–246.
- Karant H, Shenoy VS, Murthy RR. 2006. Industrially feasible alternative approaches in the manufacture of solid dispersions: A technical report. *AAPS PharmSciTech* 7:E1–E8.
- Craig DQM. 2002. The mechanisms of drug release from solid dispersions in water-soluble polymers. *Int J Pharm* 231:131–144.
- Kerč J, Srčič S, Kofler B. 1998. Alternative solvent-free preparation for felodipine surface solid dispersions. *Drug Dev Ind Pharm* 24:359–363.
- Fini A, Moyano JR, Gines JM, Perez-Martinez JI, Rabascon AM. 2005. Diclofenac salts, II. Solid dispersions in PEG6000 and Gelucire 50/13. *Eur J Pharm Biopharm* 60:99–111.
- Serajuddin ATM. 1999. Solid dispersion of poorly water-soluble drugs: Early promises, subsequent problems, and recent breakthroughs. *J Pharm Sci* 88:1058–1066.
- Liu C, Deasi KG. 2005. Characteristics of rofecoxib-polyethylene glycol 4000 solid dispersion and tablets based on solid dispersions. *Pharm Dev Technol* 10:467–477.
- Narang AS, Srivastava AK. 2002. Evaluation of solid dispersions of clofazimine. *Drug Dev Ind Pharm* 28:1001–1013.
- Okonogi S, Puttipatkhachorn S. 2006. Dissolution improvement of high drug-loaded solid dispersion. *AAPS PharmSciTech* 7:1–6.
- Nazzal S, Guven N, Reddy IK, Khan MA. 2002. Preparation and characterization of coenzyme Q10-Eudragit solid dispersion. *Drug Dev Ind Pharm* 28:49–57.
- Thybo P, Pedersen BL, Hovgaard L, Holm R, Mullertz A. 2008. Characterization and physical stability of spray dried solid dispersions of probucol and PVP-K30. *Pharm Dev Technol* 13:375–386.
- Thybo P, Kristensen J, Hovgaard L. 2007. Characterization and physical stability of tolfenamic acid-PVP K30 solid dispersions. *Pharm Dev Technol* 12:43–53.
- Chaulang G, Patel P, Hardikar S, Kelhar M, Bhosale A, Bhise S. 2009. Formulation and evaluation of solid dispersions of furosemide in sodium starch glycolate. *Trop J Pharm Res* 8:43–51.
- Chaulang G, Patil K, Ghodke D, Khan S, Yeole P. 2008. Preparation and characterization of solid dispersion tablet of furosemide with crospovidone. *Res J Pharm Technol* 1:386–389.
- Gillies ER, Frechet JMJ. 2005. Dendrimers and dendritic polymers in drug delivery. *Drug Discov Today* 10:35–43.

25. Žagar E, Žigon M. 2002. Characterization of a commercial hyperbranched aliphatic polyester based on 2,2-bis(methylol)propionic acid. *Macromolecules* 35:9913–9925.
26. Žagar E, Huskić M, Žigon M. 2007. Structure-to-properties relationship of aliphatic hyperbranched polyesters. *Macromol Chem Phys* 208:1379–1387.
27. Florence AT. 2005. Dendrimers: a versatile targeting platform. *Adv Drug Deliv Rev* 15:2104–2105.
28. Kolhe P, Misra E, Kannan RM, Kannan S, Lieh-Lai M. 2003. Drug complexation, *in vitro* release and cellular entry of dendrimers and hyperbranched polymers. *Int J Pharm* 259:143–160.
29. Mishra MK, Kobayashi S. 1999. *Star and hyperbranched polymers*. 1st ed. New York: Marcel Dekker.
30. Fréchet JMJ. 1994. Functional polymers and dendrimers: Reactivity, molecular architecture, and interfacial energy. *Science* 263:1710–1715.
31. Hult A, Johansson M, Malmström E. 1999. Hyperbranched polymers. *Adv Polym Sci* 143:1–34.
32. Sunder A, Heinemann J, Frey H. 2000. Controlling the growth of polymer trees: Concepts and perspectives for hyperbranched polymers. *Chemistry* 6:2499–2506.
33. Žagar E, Žigon M. 2011. Aliphatic hyperbranched polyesters based on 2,2-bis(methylol)propionic acid—Determination of structure, solution and bulk properties. *Prog Polym Sci* 36:53–88.
34. Duncan R, Izzo L. 2005. Dendrimer biocompatibility and toxicity. *Adv Drug Del Rev* 57:2215–2237.
35. Reven S, Grdadolnik J, Kristl J, Žagar E. 2010. Hyperbranched poly(esteramides) as solubility enhancers for poorly water-soluble drug glimepiride. *Int J Pharm* 396:119–126.
36. Grbic S, Parojic J, Malenovic A, Djuric Z, Maksimovic M. 2010. A contribution to the glimepiride dissociation constant determination. *J Chem Eng Data* 55:1368–1371.
37. Frisch MJ, Trucks GW, Schlegel HB, Scuseria GE, Robb MA, Cheeseman JR, Montgomery Jr. JA, Vreven T, Kudin KN, Burant JC, Millam JM, Iyengar SS, Tomasi J, Barone V, Mennucci B, Cossi M, Scalmani G, Rega N, Petersson GA, Nakatsuji H, Hada M, Ehara M, Toyota K, Fukuda R, Hasegawa J, Ishida M, Nakajima T, Honda Y, Kitao O, Nakai H, Klene M, Li X, Knox JE, Hratchian HP, Cross JB, Bakken V, Adamo C, Jaramillo J, Gomperts R, Stratmann RE, Yazyev O, Austin AJ, Cammi R, Pomelli C, Ochterski JW, Ayala PY, Morokuma K, Voth GA, Salvador P, Dannenberg JJ, Zakrzewski VG, Dapprich S, Daniels AD, Strain MC, Farkas O, Malick DK, Rabuck AD, Raghavachari K, Foresman JB, Ortiz JV, Cui Q, Baboul AG, Clifford S, Cioslowski J, Stefanov BB, Liu G, Liashenko A, Piskorz P, Komaromi I, Martin RL, Fox DJ, Keith T, Al-Laham MA, Peng CY, Nanayakkara A, Challacombe M, Gill PMW, Johnson B, Chen W, Wong MW, Gonzalez C, Pople JA. Gaussian 03, Revision C.02. Wallingford, Connecticut: Gaussian Inc.
38. Becke AD. 1993. Density-functional thermochemistry. 3. The role of exact exchange. *J Chem Phys* 98:5648–5652.
39. Lee C, Yang W, Parr RG. 1988. Development of the Colle-Salvetti correlation-energy formula into a functional of the electron density. *Phys Rev B Condens Matter* 37:785–789.
40. Florian J, Warshel A. 1997. Langevin dipoles model for *ab initio* calculations of chemical processes in solution: Parameterization and application to hydration free energies of neutral and ionic solutes and conformational analysis in aqueous solution. *J Phys Chem* 101:5583–5595.
41. Borštnar R, Roy Choudhury A, Stare J, Novic M, Mavri J. 2010. Calculation of pKa values of carboxylic acids: Application to bilirubin. *J Mol Struct THEOCHEM* 947:76–82.
42. Žagar E, Huskić M, Grdadolnik J, Žigon M, Zupančič-Valant A. 2005. Effect of annealing on the rheological and thermal properties of aliphatic hyperbranched polyester based on 2,2-bis(methylol)propionic acid. *Macromolecules* 38:3933–3942.
43. Bellamy LJ. 1975. *The infrared spectra of complex molecules*, 3rd ed. London: Chapman and Hall, p 266.
44. Reven S, Homar M, Peternel L, Kristl J, Žagar E. Preparation and characterization of tablet formulation based on solid dispersion of glimepiride and poly(ester amide) hyperbranched polymer. *Pharm Dev Technol* (submitted).